Supplementary Information (SI) for Green Chemistry.

Electronic Supplementary Information

Synthesis of CO_2-based biomass non-isocyanate polyurethanes hybrid adhesives with excellent mechanical property and water resistance

Ping Zhang[a], Chen Qin[a], Hao Yuan[a], Yu Wang[a], Yizhong Cao[a], Zhe Wang[a,*], Chunde Jin[a,*]

[a] Bamboo Industry Institute, Zhejiang A & F University, Hangzhou 311300, PR China.

* Corresponding author: Zhe Wang, E-mail: wangzhe@zafu.edu.cn; Chunde Jin, E-mail: jincd@zafu.edu.cn

Contents

Materials and Reagents

The enzymatic hydrolysis lignin (EHL) was provided by Shandong LongLi Biotechnology Co., Ltd. (Shandong, China). Ethanol and NaOH were supplied by Sinopharm Co., Ltd. (China). The epichlorohydrin and N, N-Dimethylacetamide (DMAC) were purchased from Aladdin Co., Ltd. (China). Tetramethylammonium chloride (TMAC, purity >98 %) was provided by Macklin Biochemical Technology Co., Ltd. (Shanghai, China). Cashew phenol glycidyl ether (602A) was obtained from Nasurfar Biomaterials Technology Co., Ltd. (Changshu, China). Priamine 1074 (total amine: 208 mg KOH g^{-1}) was provided from Croda, U.K. CO_2 (≥ 99%) was purchased from Nanjing Max Special Gas Co., Ltd. Benzyl triethylammonium chloride (TEBA) was acquired from Macklin Biochemical Technology Co., Ltd. (Shanghai, China). The seawater used was acquired from Zhoushan, Zhejiang province, China. All chemicals were of analytical grade and used without further purification.

Determination of the epoxy value

The process for determining the epoxy value of CPCC by the hydrochloric acid-acetone method is as follows.

1) This mixed indicator solution was obtained by mixing 0.1% cresol red solution and 0.1% thymol blue solution in a volume ratio of 1:3, and then adjusting the mixed indicator solution to neutrality with 0.1 mol L^{-1} NaOH solution.

2) After adding the test sample with precise mass (accuracy of 0.0001 g) and 20 mL hydrochloric acid-acetone solution with a volume ratio of 1:40 in a 250 mL conical flask, the conical flask was then sealed and shaken to ensure the sample was fully

dissolved.

3) After placing the conical flask in the dark for 30 min, the aforementioned mixed solution was added 0.5 mL mixed indicator solution and titrated with 0.1 mol L^{-1} NaOH standard solution until it turned blue-purple and did not fade within 30 seconds. Additionally, the blank titration experiment was performed using the same method.

The epoxy value (*E*) is calculated according to Equation (1):

$$E = \frac{(V_1 - V_2) \times C}{10m} \tag{1}$$

Where, V_1 represents the volume of NaOH standard solution consumed in the blank test (mL); V_2 refers to the volume of NaOH standard solution consumed in the sample test (mL); m represents the mass of the sample (g); *C* represents the concentration of NaOH standard titration solution (mol L^{-1}).

Characterization

GPC, FTIR and ^{1}H NMR spectrum analysis

The functional groups of the samples were analyzed using a Fourier transform infrared spectrometer (FTIR, Magna-IR 560, Nicolet, USA) with the scanning range spanning from 450 to 4000 cm^{-1}. The molecular weight (M_W) and molecular weight distribution of EHL, EFL, and LEP following acetylation were measured using Gel Permeation Chromatography (GPC, Agilent 1200 series, Agilent Technologies, Santa Clara, US), with tetrahydrofuran serving as the mobile phase.

The acetylation process was executed as follows: 200 mg lignin samples were dissolved in 8 mL pyridine/acetic anhydride (1:1, v/v) mixed solution. Subsequently, the mixture was stirred at room temperature under light-protected conditions for 2 h.

Small amounts of ethanol were then added repeatedly to reaction system, and rotary evaporation was performed to remove the excess acetic anhydride and pyridine. After concentration, the mixture was introduced to an acidic aqueous solution (10 times the volume) to precipitate the lignin. Finally, the acetylated lignin was stored after freeze-drying.

The quantitative analysis of the epoxy groups in LEP was performed using a Nuclear Magnetic Resonance (NMR) hydrogen spectrum instrument (Avance III 400 MHz, Bruker, Germany). 30 mg LEP powder and 11.63 mg *p*-nitrobenzaldehyde were completely dissolved in 0.6 mL DMSO-d_6. The ^{1}H NMR spectrum of 602A and CPCC at varying reaction times was recorded using the Nuclear Magnetic Resonance (NMR) hydrogen spectrum instrument (Avance NEO 500 MHz, Bruker, Germany) with $CDCl_3$ as the deuterated reagent.

The 2D HSQC NMR and ^{31}P NMR analysis

The 2D HSQC NMR and ^{31}P NMR of lignin samples were tested using the Bruker 500 MHz and the samples were completely dried prior to testing. The lignin sample (25 mg) was added to DMSO-d_6 (600 μL) for the 2D HSQC NMR test with 64 scans. Before performing ^{31}P NMR spectroscopy on lignin with 64 scans, it is essential to treat it with NMR solvent. In briefly, the deuterated mixed reagent was prepared by mixing deuterated pyridine and deuterated chloroform in a volume ratio of 1.6:1. 20 mg lignin was dissolved the mixed solution with 100 uL internal standard solution, 0.5 mL deuterated mixed reagent, and 0.1 mL relaxation solution. After thorough mixing to ensure homogeneity, 0.1 mL 2-Chloro-4,4,5,5-tetramethyl-1,3,2-dioxaphospholane

(TMDP) was added the aforementioned solution and shook vigorously to ensure complete reaction for 15 min. Then the mixed reagents were transferred to an NMR tube for quantitative ^{31}P NMR analysis. The 10.85 mg mL^{-1} internal standard solution was prepared by dissolving 54.25 mg cyclohexanol to 5 mL deuterated mixed reagent. The 5 mg mL^{-1} relaxation reagent solution was prepared by dissolving 25 mg chromium acetylacetonate in 5 mL deuterated mixed reagent.

Thermal analysis

The mass loss of lignin samples and LEP-NIPU samples were analyzed on the thermogravimetric analyzer (Netzsch, TG 209 F3 Tarsus, Germany) from 30 °C to 600 °C at a heating rate of 10 °C min^{-1} in N_2 gas. The glass transition temperature (T_g) of lignin samples were tested using DSC (Q2000, TA, USA). The samples were heated from room temperature to 120 °C at a rate of 10 °C min^{-1} in N_2 atmosphere, then maintained at 120 °C for 10 min, and cooled down to room temperature for eliminating heat history. Subsequently the samples were reheated from room temperature to 200 °C again.

Dynamic Mechanical Analysis

The mechanical properties of the samples were measured using a Dynamic Mechanical Analyzer (Q800, TA, USA) over a temperature range from -50 °C to 150 °C, with a heating rate of 5°C min^{-1} and a frequency of 1 Hz.

Tensile testing of LEP-NIPU films

The LEP-NIPU films were sheared to a dumbbell shape (total length:35 mm, narrow section width:25 mm) and the tensile testing were performed using a testing machine (Instron5960, America) at 25 °C with a speed of 5 mm min^{-1}. Each sample was tested three times.

Tensile fracture surface analysis and contact angle test

The tensile fracture surface of LEP-NIPU samples were observed by Scanning Electron Microscope (SEM, SU8010, Hitachi, Japan). The water and seawater repellency of LEP-NIPU films were evaluated by their contact angles detected by OCA50AF contact angle test system (DataPhysics, Germany) at room temperature.

Supplement Table and Figures

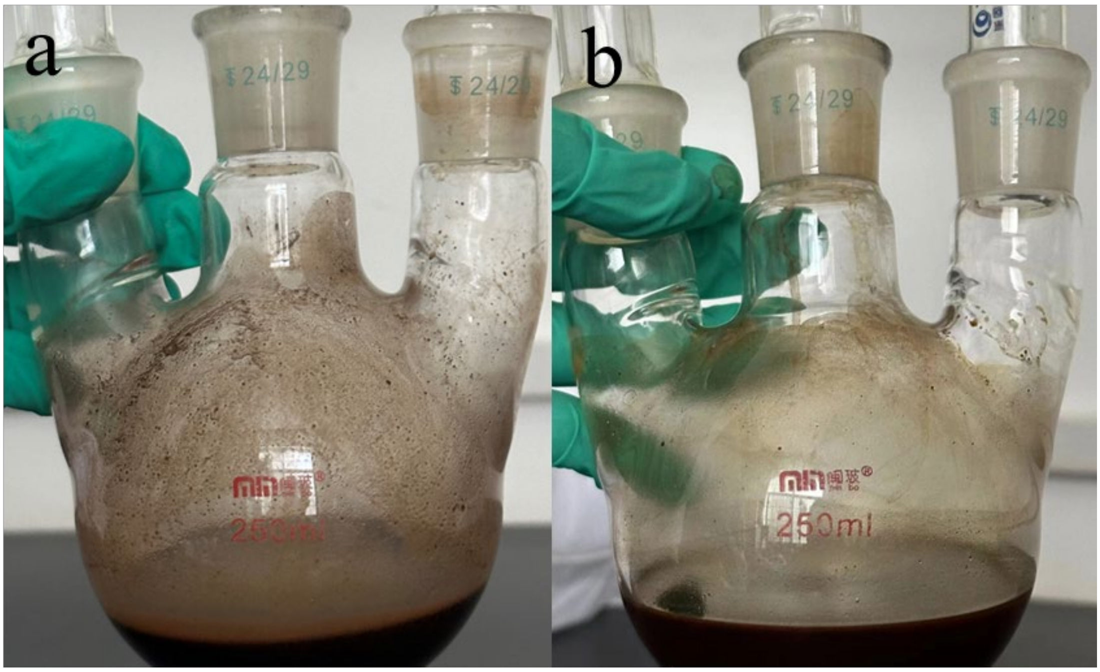

Fig. S1. Photographs of EHL and EFL dissolved in epichlorohydrin

Fig. S2. Photographs of EHL, EFL and LEP

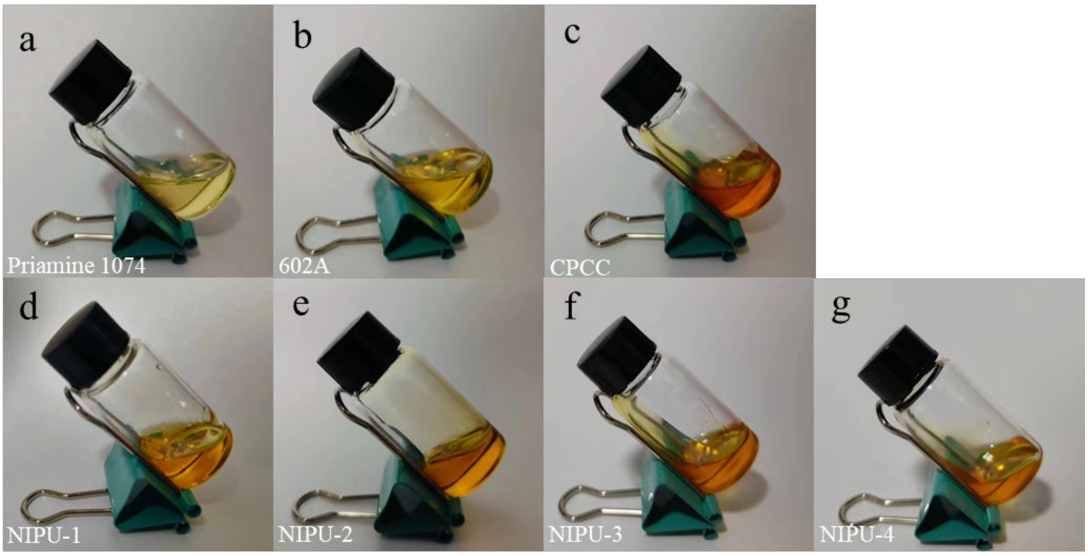

Fig. S3. Photographs of Priamine 1074, 602A, CPCC, and NIPU prepolymers

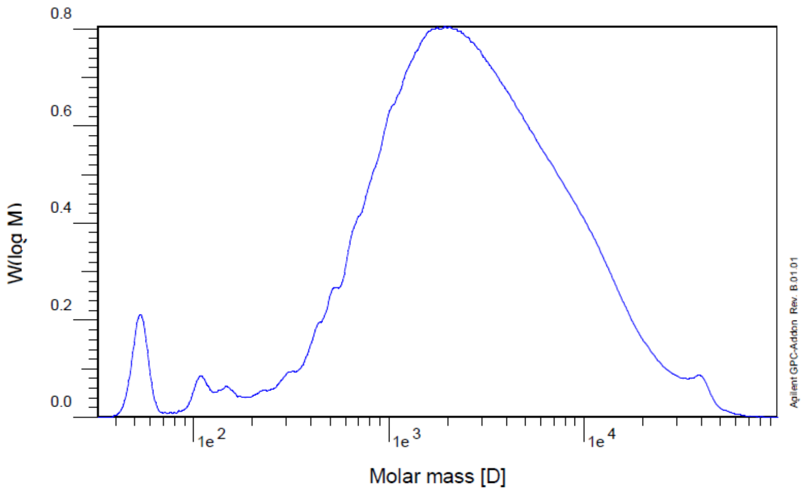

dad1A

Mn :	8.6996e2	g/mol
Mw :	4.7759e3	g/mol
Mz :	1.4186e4	g/mol
Mv :	0.000000	g/mol
D :	5.4898e0	
[n]:	0.000000	ml/g
Vp :	7.6383e0	ml
Mp :	2.3252e3	g/mol
A :	1.7045e2	ml*V
10%	5.6869e2	g/mol
30%	1.3505e3	g/mol
50%	2.4147e3	g/mol
70%	4.5754e3	g/mol
90%	1.1427e4	g/mol

Fig. S4. GPC results of EHL.

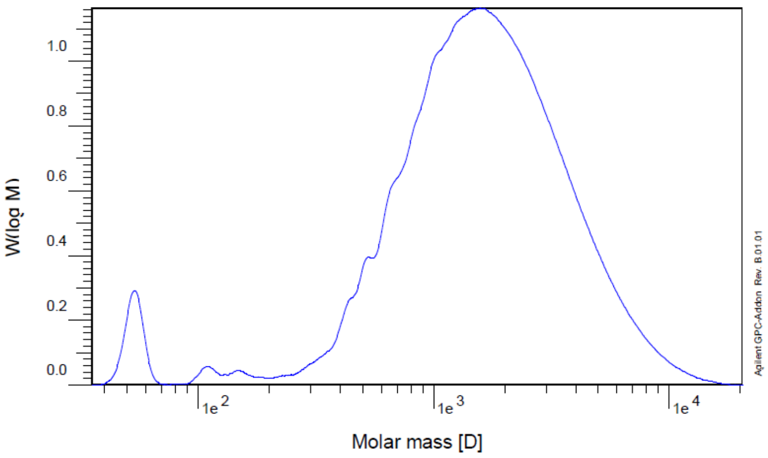

dad1A

Mn :	7.2265e2	g/mol
Mw :	2.1066e3	g/mol
Mz :	3.7135e3	g/mol
Mv :	0.000000	g/mol
D :	2.9151e0	
[n]:	0.000000	ml/g
Vp :	7.9450e0	ml
Mp :	1.6445e3	g/mol
A :	2.1951e2	ml*V
10%	5.4166e2	g/mol
30%	1.0414e3	g/mol
50%	1.5751e3	g/mol
70%	2.3871e3	g/mol
90%	4.3233e3	g/mol

Fig. S5. GPC results of EFL.

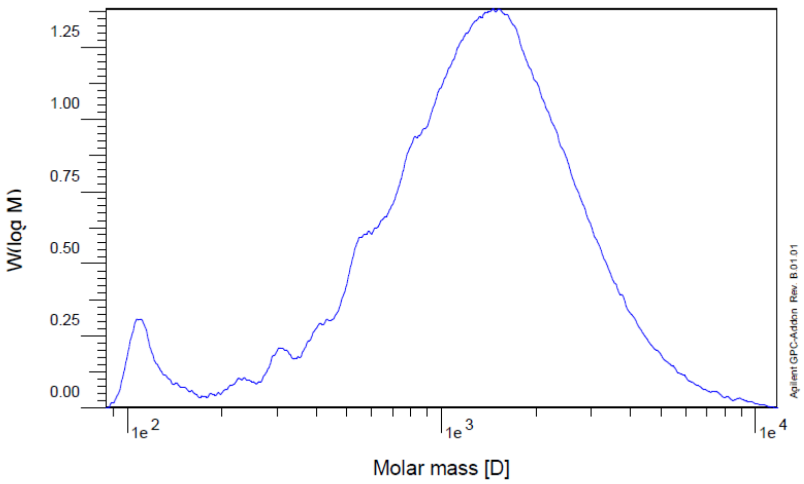

```
       dad1A

Mn :   7.9297e2      g/mol
Mw :   1.6037e3      g/mol
Mz :   2.5546e3      g/mol
Mv :   0.000000      g/mol
D  :   2.0223e0
[n]:   0.000000      ml/g
Vp :   8.0158e0      ml
Mp :   1.5204e3      g/mol
A  :   3.8090e1      ml*V
10%    4.4431e2      g/mol
30%    8.9566e2      g/mol
50%    1.3168e3      g/mol
70%    1.8551e3      g/mol
90%    3.0691e3      g/mol
```

Fig. S6. GPC results of LEP.

Table S1. Assignment of main ^{13}C-^{1}H crossing-signals in the HSQC spectra of the lignin.

Lable	δC/δH(ppm)	Assignments
C_{β}	53.3/3.46	C_{β}−H_{β} in phenylcoumaran substructures (C)
B_{β}	53.5/3.06	C_{β}−H_{β} in resinol substructures (B)
$-OCH_3$	55.6/3.73	C−H in methoxyls
A_{γ}	59.5-59.7/3.40-3.63	C_{γ}−H_{γ} in β-O-4′ substructures (A)
I_{γ}	61.4/4.10	C_{γ}−H_{γ} in p-hydroxycinnamyl alcohol end groups (I)
A'_{γ}	63.2/4.33-4.49	C_{γ}−H_{γ} in γ-acylated β-O-4′ substructures (A′)
C_{γ}	62.5/3.73	C_{γ}−H_{γ} in phenylcoumaran substructures (C)
B_{γ}	71.0/3.82 and 4.18	C_{γ}−H_{γ} in resinol substructures (B)
A_{α}	71.8/4.86	C_{α}−H_{α} in β-O-4′ substructures (A)
$A_{\beta(G/H)}$	83.9/4.29	C_{β}−H_{β} in β-O-4′ substructures linked to G/H units (A)
B_{α}	84.8/4.65	C_{α}−H_{α} in resinol substructures (B)
$A_{\beta(S)}$	85.9/4.12	C_{β}−H_{β} in β-O-4′ substructures linked to S units (A)
C_{α}	86.8/5.46	C_{α}−H_{α} in phenylcoumaran substructures (C)
$S_{2,6}$	103.8/6.71	$C_{2,6}$−$H_{2,6}$ in etherified syringyl units (S)
$S'_{2,6}$	106.2/7.23 and 7.07	$C_{2,6}$−$H_{2,6}$ in oxidized (Cα=O) syringyl units (S′)
G_2	110.9/6.98	C_2−H_2 in guaiacyl units (G)
G_5	114.9/6.77	C_5−H_5 in guaiacyl units (G)
G_6	119.0/6.80	C_6−H_6 in guaiacyl units (G)
$H_{2,6}$	127.9/7.19	$C_{2,6}$-$H_{2,6}$ in p-hydroxyphenyl units (H)
I_{β}	128.2/6.25	C_{β}−H_{β} in p-hydroxycinnamyl alcohol end groups (I)
I_{α}	128.4/6.44	C_{α}−H_{α} in p-hydroxycinnamyl alcohol end groups (I)
$pCA_{2,6}$	130.66/7.43	$C_{2,6}$−$H_{2,6}$ in *p*-coumarate substructures (*p*CA)
pCA_{α}	144.87/7.51	C_{α}−H_{α} in *p*-coumarate substructures (*p*CA)
FA_{α}	144.87/7.47	C_{α}−H_{α} in ferulate substructures (FA)

Table S2. The results of 2D-HSQC spectra of the lignin.

	S	G	H	S/G	β-O-4	β-5
EHL	33.84%	64.25%	1.91%	0.53	7.38%	0.62%
EFL	32.41%	66.55%	1.04%	0.49	3.96%	0.74%
LEP	16.04%	83.60%	0.36%	0.19	2.36%	0.42%

Fig. S7. Photographs of LEP-NIPU$_{50:50}$ film successfully lifting a 1.5 kg object.

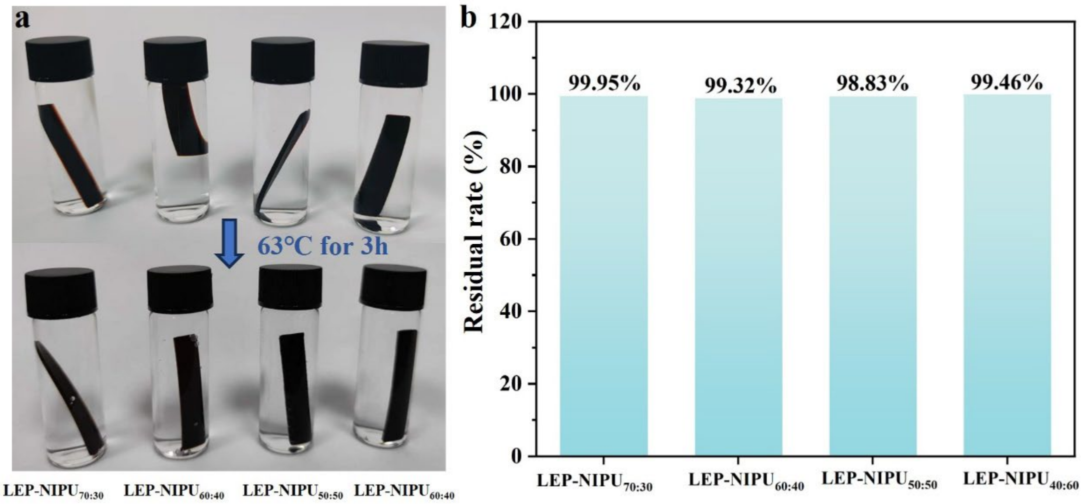

Fig. S8. (a) Photographs and (b) residual rate of LEP-NIPUs films boiling at 63 °C for 3 h.

Table S3. The curing characteristic parameters of LEP-NIPUs samples at different heating rates.

Sample	β (K/min)	T_i	T_p	T_f
LEP-NIPU $_{60:40}$	5	353.15	382.13	406.14
	10	355.15	393.77	420.11
	15	358.15	401.09	426.09
	20	360.15	406.53	433.55
	25	364.15	411.93	438.35
LEP-NIPU $_{50:50}$	5	360.15	396.18	419.84
	10	361.65	407.08	429.79
	15	363.15	415.99	443.88
	20	364.15	422.54	445.23
	25	365.15	426.97	454.03
LEP-NIPU $_{40:60}$	5	361.15	401.7	423.70
	10	362.05	413.91	436.35
	15	363.15	422.15	449.77
	20	366.15	428.36	457.6
	25	366.75	434.05	461.92
LEP-NIPU $_{30:70}$	5	363.15	412.44	435.25
	10	364.15	426.71	448.52
	15	365.15	432.32	439.65
	20	365.85	437.28	448.95
	25	367.25	444.82	455.1

Table S4. The E_a, A, and R^2 parameters acquired by Kissinger and Ozawa approach.

Sample	**Kissinger**[a]			**Ozawa**[b]	
	E_a **(kJ/mol)**	A **(s^{-1})**	R^2	E_a **(kJ/mol)**	R^2
LEP-NIPU$_{30:70}$	68.16	1.04×10^8	0.9988	75.28	0.9990
LEP-NIPU$_{40:60}$	66.36	1.03×10^8	0.9922	73.31	0.9937
LEP-NIPU$_{50:50}$	65.59	1.16×10^8	0.9883	72.43	0.9906
LEP-NIPU$_{60:40}$	63.47	1.28×10^8	0.9955	70.07	0.9965

a: Kissinger equation:

$$ln\ (\beta/{T_P}^2) = ln\ (AR/E_a) - E_a/RT_P \qquad (1)$$

Where β, A, T_p, R and E_a represent the heating rate, preexponential factor, peak temperature, gas constant (8.314 J mol^{-1} K^{-1}) and apparent activation energy, respectively.

b: Ozawa equation:

$$ln\beta = -5.331 - 1.052((E_a/R\,T_P) + ln(AE_a/R) - lnf(\alpha)) \qquad (2)$$

Where β, T_p, R and E_a indicate the heating rate, peak temperature, gas constant (8.314 J mol^{-1} K^{-1}) and apparent activation energy, respectively.

Table S5. The kinetic models of curing reaction of LEP-NIPUs samples.

Sample	**Dynamic modeling**
LEP-NIPU$_{60:40}$	$\frac{d\alpha}{dt} = 1.28 \times 10^8 (1-\alpha)^{0.9059} \exp(-\frac{63.47}{RT_P})$
LEP-NIPU$_{50:50}$	$\frac{d\alpha}{dt} = 1.16 \times 10^8 (1-\alpha)^{0.9056} \exp(-\frac{65.59}{RT_P})$
LEP-NIPU$_{40:60}$	$\frac{d\alpha}{dt} = 1.03 \times 10^8 (1-\alpha)^{0.9052} \exp(-\frac{66.36}{RT_P})$
LEP-NIPU$_{30:70}$	$\frac{d\alpha}{dt} = 1.04 \times 10^8 (1-\alpha)^{0.9045} \exp(-\frac{68.16}{RT_P})$

Table S6. The curing temperature and time of LEP-NIPUs samples.

Sample	**Curing temperature (°C)**	**Curing time (min)**
LEP-NIPU$_{60:40}$	104.23	305.6
LEP-NIPU$_{50:50}$	117.49	325.7
LEP-NIPU$_{40:60}$	123.14	347.4
LEP-NIPU$_{30:70}$	134.97	324.6

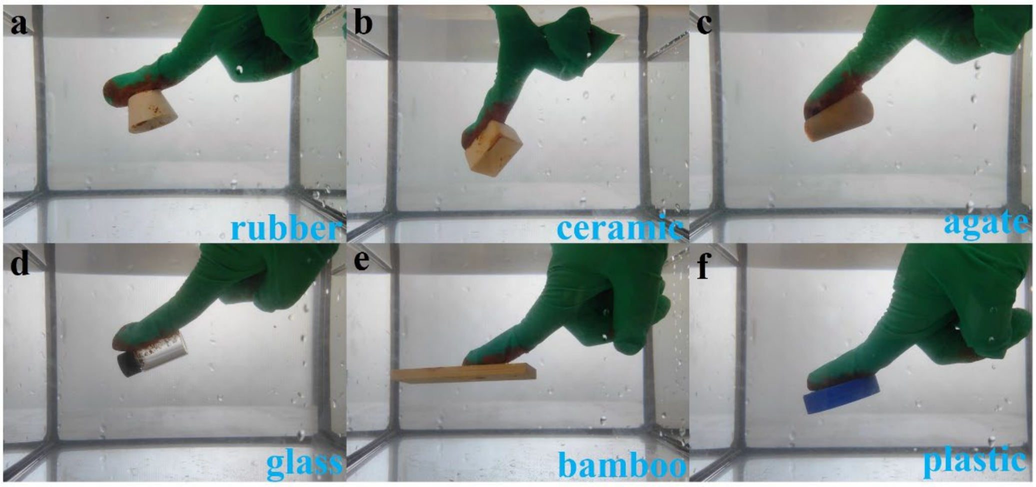

Fig. S9a-f. Photographs of the LEP-NIPU$_{60:40}$ adhesives adhered with different substrate materials under seawater.

LCA assessment

To demonstrate the greenness of the utilized biomass prepolymers, the life cycle assessment (LCA) was carried out on both the self-synthesized NIPU prepolymers in this thesis and the petroleum-based NIPUs materials referred to this thesis[1]. The LCA calculation was conducted utilizing the eFootprint and referred to the guidelines in ISO 14044. The ecoinvent database v.3.0 and CLCD were utilized to obtain all data in the life cycle inventory (LCI)[2,3]. In this context, the LCA report considered the environmental impacts during the production processes of both biomass-based and petroleum-based NIPUs. The environmental concerns encompass global warming, ozone formation, terrestrial acidification, freshwater eutrophication, marine eutrophication, terrestrial ecotoxicity, freshwater ecotoxicity, marine ecotoxicity, mineral resource scarcity, fossil resource scarcity, ionizing radiation, fine particulate matter formation, human carcinogenic toxicity, human non-carcinogenic toxicity, land use, water consumption, and so forth. It can be illustrated from **Fig. 1** that the carbon emission of biomass-based NIPUs was 31.06 kg CO_2 eq, which was lower than that of petroleum-based NIPUs. Besides, the biomass-based NIPUs exhibits lower trends in fossil resource scarcity, terrestrial ecotoxicity, terrestrial acidification, fine particulate matter formation, and ozone formation compared to the petroleum-based NIPUs. The evaluation results demonstrate that the environmental impact of the biomass-based NIPUs fabricated in this research is considerably less than that of the conventional petroleum-based NIPUs, which can illustrate that biomass-based NIPUs are more environmentally friendly than petroleum-based NIPUs.

Reference

1 J. Ke, X. Li, F. Wang, S. Jiang, M. Kang, J. Wang, Q. Li and Z. Wang, *RSC Adv.*, 2017, **7**, 28841–28852.

2 M. Chen, Y. Liu, J. Pan, Y. Jiang, X. Zou and Y. Wang, *Chem. Eng. J.*, 2024, **502**, 157993.

3 D. Costa, J. Serra, P. Quinteiro and A. C. Dias, *J. Cleaner Prod.*, 2024, **444**, 140955.

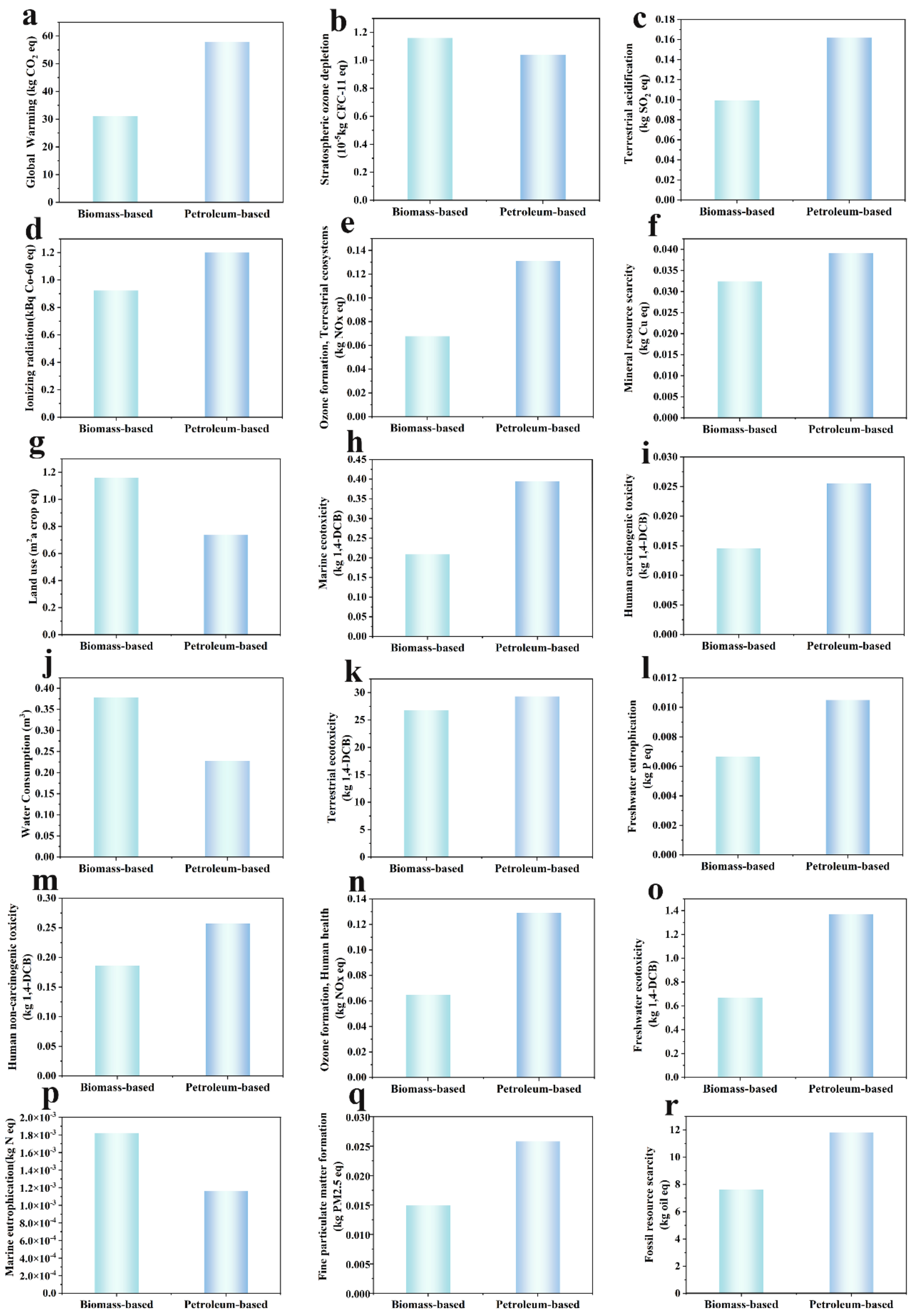

Fig. 10. (a-r) Life cycle assessment of 1 kg biomass-based and 1 kg petroleum-based NIPUs.

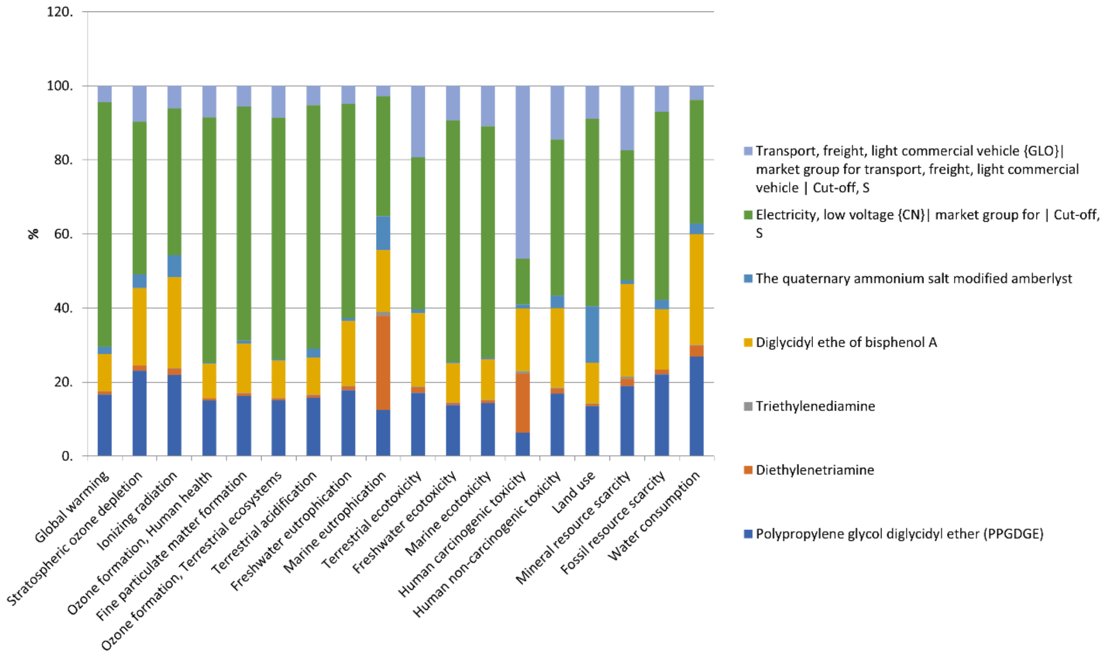

Fig. 11. Life cycle assessment of 1 kg petroleum-based NIPUs (Relative contribution).

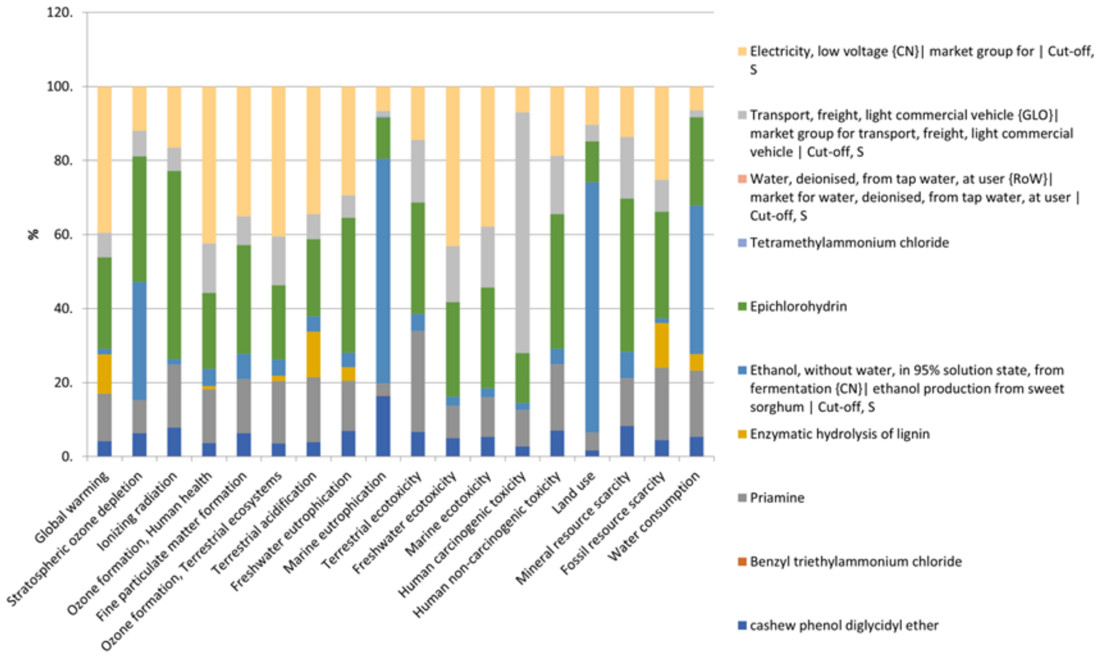

Fig. 12. Life cycle assessment of 1 kg biomass-based NIPUs (Relative contribution).